Heliyon 9 (2023) e13076

Contents lists available at ScienceDirect

Heliyon

journal homepage: www.cell.com/heliyon

Research article

Ribosomal protein L31 (RPL31) inhibits the proliferation and migration of gastric cancer cells

Fang Wu [a], Yangyang Liu [a], Shenglin Hu [c], Canrong Lu [b,*]

[a] Department of Oncology, The First Affiliated Hospital of Nanchang University. Yongwaizheng Street, No. 17, Nanchang City, Jiangxi Province 330006, China
[b] Senior Department of General Surgery, The First Medical Center of Chinese, PLA General Hospital. Fuxin Road, No. 28, Haidian District, Beijing 100853, China
[c] Department of Internal Medicine, People's Hospital of Jinan County. Beida Street, No. 5, Jinan City, Jiangxi Province 330699, China

ARTICLE INFO

Keywords:
Gastric cancer
RPL31
Cell migration
Tumor growth
JAK-STAT pathway

ABSTRACT

Gastric cancer (GC) is a digestive tract malignant tumor and causes the third cancer-related mortality in the world. Aberrant expression of Ribosomal Protein L31 (RPL31) has been reported in several human cancers. The aim of this study was to explore the role and possible biological functions of RPL31 in GC. We firstly employed immunohistochemistry to examine RPL31 expression in tumor and para-cancerous tissues. By lentiviral transfection, we successfully constructed an RPL31-knockdown GC cell model and performed functional validation to reveal the effects of RPL31 on proliferation, apoptosis, cycle, migration, and tumor growth. Our data indicated that RPL31 was abundantly expressed in GC tissues and cell lines (AGS and MGC-803). In addition, RPL31 expression was positively correlated with the extent of tumor infiltrate of GC patients. Functionally, silencing RPL31 in AGS and MGC-803 cells significantly limited the ability of proliferation and migration, promoted cell apoptosis. Consistently, RPL31-knockdown GC cells inhibited the growth of xenografts in mice. Moreover, preliminary analysis on the downstream regulation mechanism revealed that RPL31 functioned as a tumor promoter through targeting JAK-STAT signaling pathway. In conclusion, inhibition of abnormally high expression of RPL31 in GC may be a potential therapeutic strategy for this disease.

1. Introduction

As a significant malignancy, gastric cancer (GC) remains a serious public health problem worldwide. In basis of American Cancer Society, the most recent estimates in 2021 is 26,560 new cases and 11,180 deaths from GC in the United States [1]. It accounts for 8.2% of the cancer-related deaths and is the third leading cause all around the world [2], primarily due to the lack of specific molecular biomarkers providing effective early detection as GC processes. Moreover, it is hard to detect in the early stage of tumor progression but has been characterized by early metastasis, poor prognosis and frequent recurrence which leads to low survival rate within five years and high mortality [3]. Even more seriously is that the median overall survival rate of patients suffering from metastatic GC is mostly less than 1 year [4]. Multiple risk factors could induce GC, including both environmental and genetic influence factors (e.g., diet, smoking, excessive alcohol consumption and Epstein-Barr virus infection) [5]. Nowadays, the traditional therapeutic methods are

* Corresponding author.
E-mail address: lucanrong@301hospital.com.cn (C. Lu).

https://doi.org/10.1016/j.heliyon.2023.e13076
Received 16 November 2022; Received in revised form 4 January 2023; Accepted 16 January 2023
Available online 20 January 2023

involved in surgery, chemotherapy and radiotherapy. Recently, with the progress of biological technology, new treatments for GC are gradually being applied, especially immunotherapy and targeted therapy. For instance, biomarkers, particularly microsatellite instability (MSI), programmed cell death ligand 1 (PD-L1), human epidermal growth factor Receptor 2 (HER2), tumor mutation load, and Epstein-Barr virus, are increasingly driving systemic therapeutic approaches and allowing the identification of populations most likely to benefit from immunotherapy and targeted therapies [6]. Moreover, targeted therapies including trastuzumab, navulizumab and parbolizumab have yielded encouraging results in clinical trials in patients with locally advanced or metastatic disease [7]. Nonetheless, effective diagnosis and treatment of GC patients is still a noticeable problem encountered by clinicians and scientists [8]. Therefore, a novel biomarker is necessarily required for early diagnosis and treatment of GC patients.

Ribosomal Protein L31 (RPL31, also known as L31; Gene ID: 6160) belongs to the ribosomal protein L31E family, which is a part of the 60 S large ribosomal subunit, located on human chromosome 2 (2q11.2), and regulates a variety of physiological and pathological processes in the cytoplasm [9–11]. RPL31 has been shown to be involved in ribosome self-assembly, protein synthesis, cell proliferation, DNA repair, and tumorigenesis [9–11]. For example, the expression of HL31, which is highly homologous to eL31, is increased in colorectal tumors [12]. Moreover, Shu et al. reported that RPL31 was one of the six genes in nasopharyngeal carcinoma through screening tumor antigen genes in the cDNA library [13]. Although the recombinant RPL31 protein from the giant panda exhibited inhibition of cell growth and anti-cancer functions [14], clinical studies indicated that RPL31 played a tumor-promoting role in human malignancies. Sharen et al. indicated that RPL31 knockdown restricted the proliferation, migration and colony formation of CRC cells, while enhancing apoptosis [15]. Furthermore, Maruyama et al. demonstrated that RPL31 is involved in the proliferation of bicalutine-resistant prostate cancer cells [16]. However, the expression, function and prognostic correlation of RPL31 in human gastric cancer have not been revealed.

In the present study, we examined the expression of RPL31 through collecting the clinical samples and explored its biological functions *in vitro* and *in vivo* via RPL31-knockdown cell models. In addition, we preliminarily detected the underlying molecular mechanisms in cell growth and apoptosis in GC cell lines, which provided a certain theoretical basis of early diagnosis and treatment for GC patients.

2. Materials and methods

2.1. Clinical samples and immunohistochemistry (IHC) assay

Tissue microarrays of GC ($N = 123$) and para-cancerous samples ($N = 131$) were used for evaluating RPL31 expression. The collection and usage of patients' samples had been approved with permission, which followed International Ethical Guidelines for Biomedical Research Involving Human Subjects proposed by Council for International Organization of Medical Sciences (CIOMS). The histopathological grading of GC tissue microarrays here was based on the 8th Edition of the AJCC TNM Staging System [17]. Regarding IHC assay, all slides were firstly baked in oven at 65 °C for half an hour and then dewaxed and rinsed for a few times. We subsequently disposed the slides using citric acid buffer to retrieve antigen, followed by adding H_2O_2 to block the slides. Next, RPL31 antibody (1:30, Cat. # ab103991, Abcam, Cambridge, MA, USA) was included on the slides at room temperate 1 h before adding the second antibody. Finally, the staining ended after deposed by DAB and hematoxylin. The slides were photographed under a microscope. We assigned two kinds of score each slide based on the staining intensity and the positive cell score. The staining intensity was determined by the depth of dyeing color and quantified from 0 to 3, in which 0 meant no dyeing color emerging on the slide and 1–3 were pale yellow, pale brown and dark brown, respectively. The positive cell score was from 1 to 4 when the staining percentage was more than 0%, 25%, 50% and 75%, respectively. The expression level of RPL31 was lastly confirmed by multiplying the staining intensity and the positive cell score of each slide.

2.2. Lentiviral vector construction

Human gene *RPL31* was used as the template to design three RNA interference target sequences (5'-TGGGCCAAAGGAA-TAAGGAAT-3', 5'-GCACTCAAAGAGATTCGGAAA-3', 5'-CCGAGAATACACCATCAACAT-3'), with the scramble sequence (5'-TTCTCCGAACGTGTCACGT-3') adopted as the negative control. These sequences were separately connected into cDNA and then linked to BR-V108 vector (Shanghai Yibeirui Biomedical Science and Technology Co., Ltd.) by restriction enzymes (*Age*I, *Eco*R I; Thermo Fisher Scientific, Wilmington, DE, USA) and T4 DNA ligase (Thermo Fisher Scientific). The processed vectors were then transfected into *E. coli* receptor cells (Cat. # CB104-03, TIANGEN, Beijing, China) and positive cell clones were identified by PCR. EndoFree midi Plasmid Kit (Cat. # DP117, TIANGEN) was applied to extract high purity of plasmids containing inserted interference/scramble sequence. Lastly, we co-transfected the prepared BR-V108, Helper 1.0 and Helper 2.0 plasmids into 293 T cells and successfully constructed the lentivirus.

2.3. Cell transfection

The selected cell lines (AGS and MGC-803) from the previous step were cultivated in 90% RPMI-1640 (Cat. # 10-040-CVB, Corning, NY, USA) containing 10% FBS (Cat. # 16000-044, Thermo Fisher Scientific). Cell suspension was then cultivated in the incubator with 5% CO_2 at 37 °C. We next infected cells by lentivirus (shRPL31 or shCtrl) and cultured cells for 72 h. The infection efficiency of cell lines was assessed by green fluorescent protein (GFP) expression using a fluorescence microscope.

2.4. Quantitative real-time PCR (qRT-PCR) assays

Two human GC cell lines (AGS and MGC-803) and human normal gastric mucosa cells (GES1) were prepared for extracting the total of RNA in three cell lines utilizing Trizol (Cat. # T9424-100 m, Sigma-Aldrich, St. Louis, MO, USA) and RNA concentration was detected using Nanodrop spectrophotometer (Cat. # 2000/2000C, Thermo Fisher Scientific). cDNA was obtained through RNA reverse transcription employing Hiscript QRT supermix for qPCR (+gDNA WIPER) (Cat. # R123-01, Vazyme, Nanjing, China) and then preserved at −80 °C. Subsequently, we performed PCR using AceQ qPCR SYBR Green master mix (Cat. # Q111-02, Vazyme) and got RPL31 and GAPDH (the reference control) with the primers as follows,

RPL31: 5'-GCTCAACAAAGCTGTCTGGG-3' (upstream), 5'-TTATGGGCTCTTGGCGACT-3' (downstream);

GAPDH: 5'-TGACTTCAACAGCGACACCCA-3' (upstream), 5'-CACCCTGTTGCTGTAGCCAAA-3' (downstream). The relative expression level of RPL31 was finally calculated utilizing $2^{-\Delta\Delta CT}$ method.

2.5. Western blotting

The assay was employed to examine the expression level of proteins in MGC-803 cells. Specifically, cells were prepared and washed by PBS twice, after which PBS was removed and cells were lysed with pre-cooled 1 × lysis buffer. Proteins in cells were extracted using BCA protein detection kit (Cat. # 23225, HyClone-Pierce South Logan, USA) and separated by 10% SDS-PAGE. We subsequently transferred proteins to the PVDF membrane and incubated with blocking liquid for 1 h. Primary antibodies used in this study were RPL31 (1:750, Cat. # ab229534, Abcam), Bcl-2 (1:500, Cat. # SC-7382, Santa Cruz Biotechnology), c-Myc (1:1000, Cat. # 13987 T, CST), P21 (1:750, Cat. # BS-0741 R, Bioss), p-Stat3 (1:1000, Cat. # 9134, CST), JAK1 (1:1000, Cat. # ab133666, Abcam), JAK2 (1:1000, Cat. # ab108596, Abcam), Stat3 (1:1000, Cat. # 30835, CST) and standard GAPDH (1:30000, Cat. # 60004-1-Ig, Proteintech), while the secondary antibody was the HRP-goat anti-rabbit IgG polyclonal (1:3000, Cat. # A0208, Beyotime). Lastly, the membrane was washed in TBST for three times and thereafter colored using ECL-PLUS/Kit (Cat. # RPN2232, Amersham Pharmacia Biotech, Arlington Heights, IL, USA).

2.6. Celigo cell counting assay

Cell proliferation of AGS and MGC-803 cells was examined using Celigo cell counting assay. The cells in the logarithmic growth phase were digested using trypsin. Then cell suspension with ~2000 cells was supplemented into each well of the 96-well plates which was subsequently cultured at 37 °C with 5% CO2. The plates were scanned using Celigo Image Cytometer (Nexcelom, Lawrence, MA, USA) for five consecutive days. The curve of the change multiple of the number of cells in the experimental group and the control group with time was drawn.

2.7. Flow cytometry

AGS and MGC-803 cells of each group (shRPL31 and shCtrl) were seeded in the well dishes (6 cm) and cultured until cell coverage rate was about 80%. After that, cells were washed by PBS, processed by trypsin and centrifuged for 5 min (1200 rpm). To detect cell cycles, pre-cooled ethanol (70%) was used to fix cell suspension and then removed at least 1 h later. After centrifuged and washed by PBS, cells were stained with PI staining solution (40 × PI, 2 mg/mL: 100 × RNase, 10 mg/mL: 1 × PBS = 25:10:1000) for half an hour. Then we adopted FACSCalibur (eBioscience, San Diego, USA) to detect cell cycle. As to the assessment of cell apoptosis, we stained cells using Annexin V-APC for 15 min in dark and determined the percentage of cells in each mitotic phase to calculate cell apoptotic rate.

2.8. Wound healing assay

AGS and MGC-803 cells were seeded into dishes until the next day. We scratched a line across the cell layer using a 96-wounding replicator (Cat. # VP408FH, VP scientific, Thermo Fisher Scientific) and added 0.5% FBS for cultivation (5% CO_2, 37 °C) after washing for 2–3 times. After different specific periods of time, the degree of cell migration was graphed under a fluorescence microscope according to which cell migration rate was obtained.

2.9. Transwell migration assay

AGS and MGC-803 cells were trypsinized and cell suspension in the low-serum medium was prepared. Next, we loaded cell suspension into the Transwell room which contained 30% PBS and incubated cells at room temperature. Culture medium was subsequently discarded and the cells were fixed and stained using crystal violet (0.1%) for 20 min. We lastly washed cells with PBS and took photos using a microscope.

2.10. Human phospho-kinase array

Human phospho-kinase array kit was ordered from R&D (Cat. # ARY003C, Abcam) and the assay was performed based on the manufacturer's instructions. Briefly, the prepared experimental cells were solubilized in the lysis buffer from the kit, moved to the 8-well multi-dish and incubated overnight at 4 °C on a rocking platform shaker. After rinsed with distilled water, the 8-well multi-dish

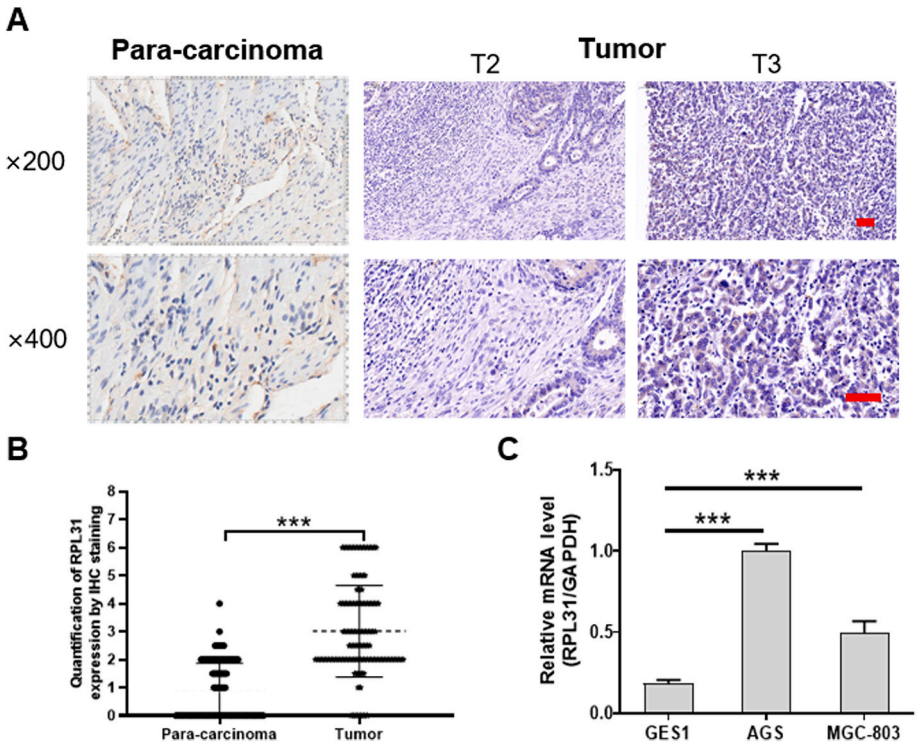

Fig. 1. The expression of RPL31 in gastric cancer (GC). (A) The negative staining in para-carcinoma tissues compared with the positive staining in tissues with different extent of tumor infiltrate. **(B)** IHC quantitative results revealed the expression of RPL31 in GC. **(C)** RPL31 expression in normal gastric mucosa cell GES1 and two GC cell lines (AGS and MGC-803), respectively. $^{***}P < 0.001$.

was then dried thoroughly. Afterward, the cell lysates were mixed with a cocktail of biotinylated detection antibodies and incubated with membranes captured with ''capture'' and control antibodies. Then, the membranes were washed, and streptavidin-horseradish peroxidase and chemiluminescent detection reagents were applied. A signal was produced at each capture spot corresponding to the amount of a phosphorylated protein bound.

2.11. Mice model construction

We purchased 20 4-week-old female BALB/c nude mice from GemPharmatech Co., Ltd. (Nanjing, China) and randomly but equally divided them into two groups (shRPL31 and shCtrl). Mice xenograft models were established after subcutaneously injected with suspension of stably-infected MGC-803 cells (5×10^7 cells/mL, 0.2 mL). Five days later, we started to weight the mice and record the length & width of the potential tumor once a week. The tumor volume was then calculated by tumor length multiplying tumor width. After five weeks from injection, the experimental animals were treated with 0.7% sodium pentobarbital (10 μL/g) and then we detected the expression of fluorescence via a PerkinElmer IVIS Spectrum imaging system. Finally, we euthanized all mice and removed the possible tumor for KI67 staining with the Primary antibody KI67 (1:150, Cat. # ab16667, Abcam) and the second antibody Goat Anti-Rabbit IgG (1:400, Cat. # ab97080, Abcam). Ethical approval was acquired from Ethics Committee of the First Affiliated Hospital of Nanchang University.

2.12. Statistical analysis

Cell experiments involved in this study were independent performed three times. The possible statistically-significant differences between two groups were detected employing Student *T* test or Sign test. Mann-Whitney *U* test and Spearman correlation analysis were adopted to assess the association between RPL31 expression level and clinical characteristics of patients. Statistics were performed in SPSS 20.0 and GraphPad Prism 7.0. Data herein were expressed as mean ± SD (standard deviation). It was considered significantly different when *P* value was less than 0.05.

Table 1
The comparison on the expression level of RPL31 between gastric cancer tissues and para-carcinoma tissues was revealed by immunohistochemistry.

RPL31 expression pattern	Tumor tissue		Para-carcinoma tissue		*P* value
	No. of cases	Percentage	No. of cases	Percentage	
Low	65	52.8%	129	98.5%	<0.001
High	58	47.2%	2	1.5%	

Table 2
The detailed information on some pathological characteristics of the patients with gastric cancer and the comparisons between expression level of RPL31 and each tumor characteristic using Mann-Whitney *U* test.

Characteristics	No. of patients	RPL31 expression pattern		*P* value
		Low	High	
All patients	123	65	58	
Age (years old)				0.883
≤64	67	35	32	
>64	56	30	26	
Gender				0.971
Male	91	48	43	
Female	32	17	15	
Tumor size				0.233
<5 cm	53	32	21	
≥5 cm	61	30	31	
Tumor infiltrate				<0.05
T1	7	7	0	
T2	17	9	8	
T3	76	41	35	
T4	23	8	15	
Lymphatic metastasis (N)				0.560
N0	21	14	7	
N1	20	8	12	
N2	29	16	13	
N3	53	27	26	
Stage				0.452
I	11	10	1	
II	34	14	20	
III	77	41	36	
IV	1	0	1	
Vessel carcinoma embolus				0.733
0	29	15	14	
1	63	35	28	
Nerve tumor infiltrates				0.872
0	36	18	18	
1	23	11	12	
Ki67 expression				0.207
<60%	50	21	29	
≥60%	61	33	28	
CD34 expression				0.914
No	18	9	9	
Yes	31	15	16	
EGFR expression				0.869
No	94	45	49	
Yes	18	9	9	
VEGF expression				0.627
No	42	19	23	
Yes	70	35	35	
CDX2 expression				0.157
No	18	6	12	
Yes	95	49	46	
Her2 expression				0.963
No	82	40	42	
Yes	29	14	15	

Note, the cut-off point (64 years old and 5 cm) was the median value of each given parameter.

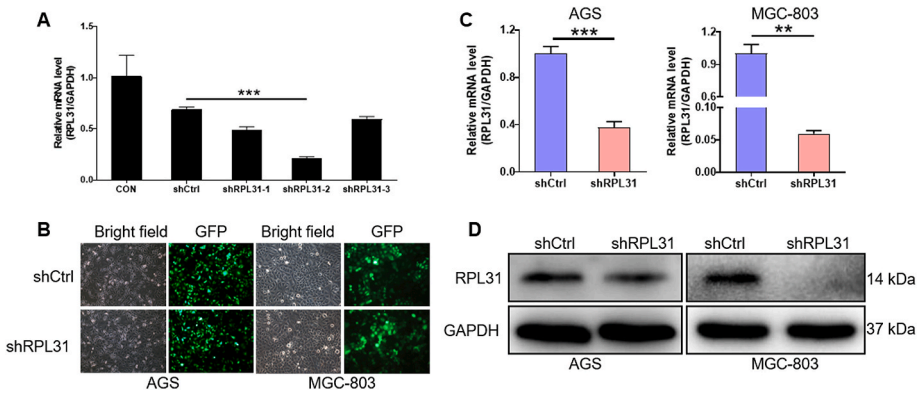

Fig. 2. The shRNA mediates stable RPL31 knockdown in GC cells. (A) Comparison of RPL31 expression in three shRNA sequences targeting RPL31 (shRPL31-1, shRPL31-2 and shRPL31-3). **(B)** The representative fluorescence microscopy images and the comparison of relative mRNA level (RPL31/GAPDH) in shRPL31 and control groups of AGS and MGC-803 cell lines. **(C–D)** The mRNA and protein expression of RPL31 in shRPL31 and shCtrl (negative control) of AGS and MGC-803 cell lines. Notably, full and non-adjusted images are available in the Supplemental materials folder. $^{**}P < 0.01$, $^{***}P < 0.001$.

3. Results

3.1. RPL31 is highly expressed in human GC

Based on clinical GC patients, 123 tumor tissues and 131 para-cancerous tissues were formed into tissue microarrays for IHC staining assay to explore RPL31 protein expression. The results showed that the expression of RPL31 in the tumor tissues was higher than that in the para-cancerous tissues (Fig. 1A). According to the IHC quantitative results, higher than the median of 3 was regarded as high expression of RPL31, otherwise it was considered low expression ($P < 0.001$, Fig. 1B). High expression of RPL31 was predominantly detected in 47.2% (58 of 123) of the tumor tissues, whereas only one case (1.5%) showed the positive staining in corresponding para-carcinoma tissues (Table 1). In addition, the expression of RPL31 in normal cell line (GES1) and GC cell lines (AGS and MGC-803) were detected, showing that RPL31 was upregulated in AGS and MGC-803 cells compared with that in GES1 cells ($P < 0.001$, Fig. 1C). As a consequence, RPL31 was highly expressed in human GC tissues and cells.

3.2. Relationship between RPL31 expression and GC pathological features

According to clinical case information of GC patients, the relationship between RPL31 expression patterns and tumor pathological features was analyzed. The results showed that the expression of RPL31 was positively correlated with the degree of tumor invasion ($P = 0.020$, Table 2). However, we failed to find significant relationship between RPL31 expression pattern and patients' age or gender. Regarding the tumor characteristics, the likelihood of highly- or low-expressed RPL31 was independent of tumor size, the extent of lymphatic metastasis, pathologic staging, whether there was vessel carcinoma embolus or nerve tumor infiltrate, or the expression of KI67, CD34, EGFR, VEGF, CDX2 or Her2 (Table 2). As a result, we suggested that RPL31 may play a key role in the evolution of GC.

3.3. The shRNA mediates stable RPL31 knockdown in GC cells

To reveal the function of RPL31 in GC cells, AGS and MGC-803 were selected to be interfered with by shRNA to steadily knock down RPL31 expression. Firstly, effective sequences of shRNA targeting RPL31 (shRPL31-2) were selected by qRT-PCR and the sequence was subsequently referred to as shRPL31 ($P < 0.001$, Fig. 2A). Subsequently, we transfected AGS and MGC-803 cell lines using lentiviruses with shRPL31 and shCtrl (scramble) sequences, respectively, and observed the transfection results under the microscope (Fig. 2B). Next, RPL31 expression was detected in AGS and MGC-803 cells after transfection with shRPL31 and shCtrl. The results of qRT-PCR revealed that the *RPL31*-knockdown efficiencies in shRPL31 groups were 62.6% in AGS cells ($P < 0.001$) and 90.1% in MGC-803 cells ($P < 0.01$), respectively (Fig. 2C). Moreover, western blotting showed that the protein level of RPL31 was downregulated in shRPL31 groups of both cell lines. Thus, the above data indicated the successful construction of *RPL31*-knockdown GC cell models.

3.4. RPL31 knockdown reduces proliferation and enhances apoptosis of GC cells

The effects of RPL31 knockdown (shRPL31) and negative control (shCtrl) GC cells on proliferation, apoptosis and cycle were tested functionally *in vitro*. Celigo cell counting assay was employed to determine the circumstance of cell growth and the outcomes disclosed that cell proliferation rates in shRPL31 groups considerably lowered in comparison with the negative controls in both cell lines (AGS cells, fold change $= -9.9$, $P < 0.001$; MGC-803, fold change $= -3$, $P < 0.001$) (Fig. 3A). Moreover, the extent of cell apoptosis was examined by flow cytometry, which demonstrated that the RPL31 knockdown resulted in much higher percentage of cell apoptosis

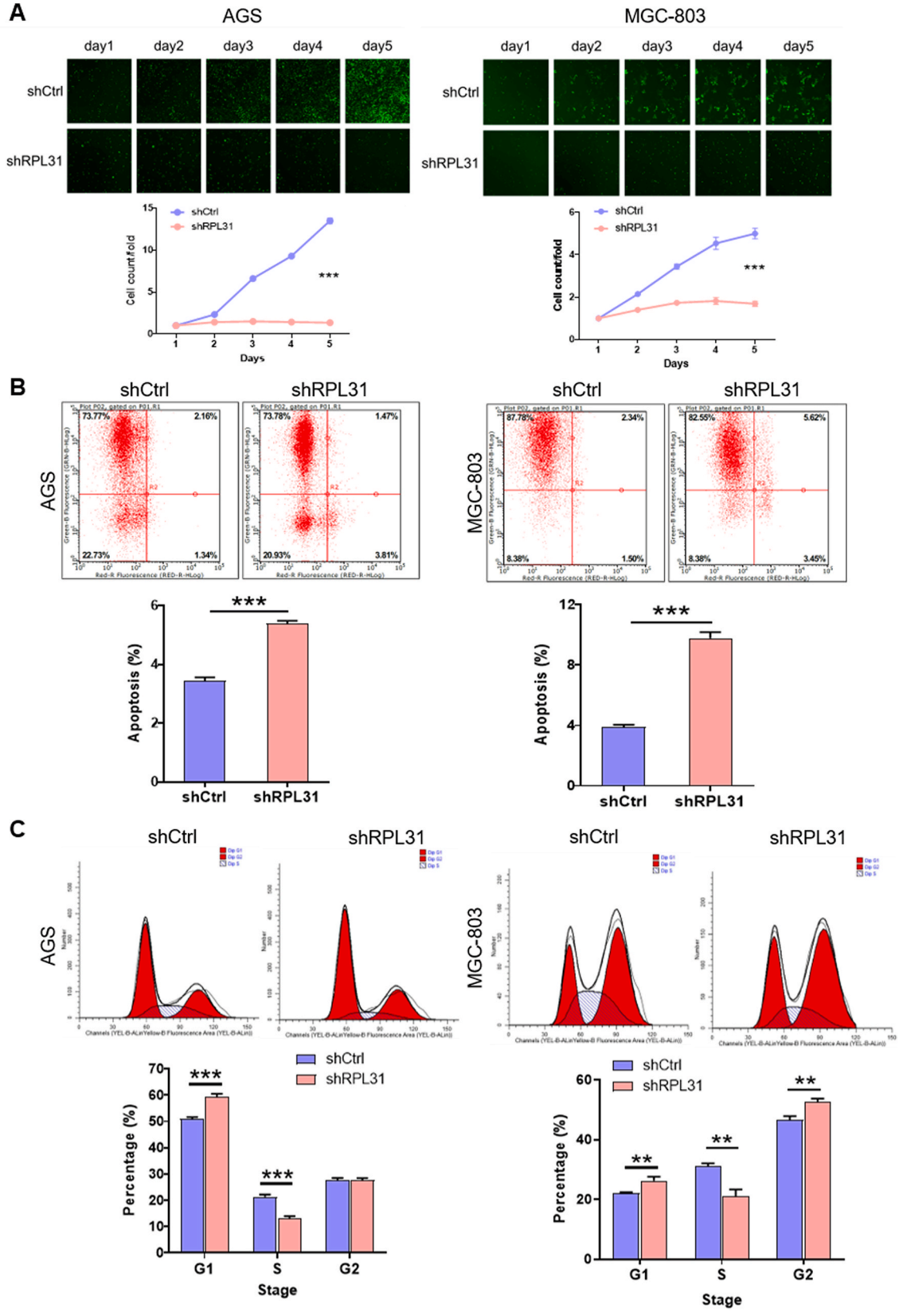
A
AGS
MGC-803
day1
day2
day3
day4
day5
shCtrl
shRPL31
Cell count/fold
Days
***
B
AGS
MGC-803
shCtrl
shRPL31
73.77%
2.16%
22.73%
1.34%
73.78%
1.47%
20.93%
3.81%
87.78%
2.34%
8.38%
1.50%
82.55%
5.62%
8.38%
3.45%
Apoptosis (%)
C
Percentage (%)
G1
S
G2
Stage
**

Fig. 3. RPL31 knockdown reduces proliferation and enhances apoptosis of GC cells. (A) The ability of cell proliferation in shRPL31-harboring and negative groups of AGS and MGC-803 cell lines resulted from Celigo cell counting assay. **(B)** The percentages of cell apoptosis obtained by flow cytometry in shRPL31-harboring and negative groups of AGS and MGC-803 cell lines. **(C)** The percentages of experimental cells in each stage in shRPL31-harboring and negative groups of AGS and MGC-803 cell lines. $^{**}P < 0.01$, $^{***}P < 0.001$.

than controls in both experimental cell lines (AGS cells, fold change = 1.6, $P < 0.001$; MGC-803, fold change = 2.5, $P < 0.001$) (Fig. 3B). In addition, flow cytometry was applied for detecting cell cycle and we found that cells in G1 phrase in the shRPL31 group were significantly more in experimental cells (AGS cells, $P < 0.001$; MGC-803, $P < 0.01$) than the negative controls, but S-stage cells in shRPL31-harboring groups were much less than cells in shCtrl-harboring groups (AGS cells, $P < 0.001$; MGC-803, $P < 0.01$). However, shRPL31 transfection led to a larger number of cells in G2 stage of MGC-803 cells ($P < 0.01$) but did not exert an influence on the number of G2-stage AGS cells (Fig. 3C). Therefore, these results illustrated that RPL31 knockdown inhibited cell malignant progression by reducing proliferation, enhancing apoptosis, and disrupting the cycle.

3.5. RPL31 knockdown inhibits GC cell migration

Subsequently, we tested and quantified the ability of cell migration using wound-healing assay and Transwell assay. As showed in Fig. 4A, silencing *RPL31* significantly slowed down the migration rates by 56% during 0–24 h in AGS cells ($P < 0.001$). As expected, similar cases were observed in MGC-803 cells, RPL31 knockdown resulted in a substantial reduction by 33% in cell migration rates during 0–48 h ($P < 0.01$). Furthermore, Transwell assay indicated that knocking down *RPL31* inhibited the movement of AGS cells by 30% ($P < 0.001$) and MGC-803 cells by 67% ($P < 0.001$) compared with the negative controls (Fig. 4B). Collectively, depletion of RPL31 greatly restrained migration in GC cell lines.

3.6. Underlying mechanisms of RPL31-mediated tumor progression

We next preliminarily explored downstream regulation of RPL31 in human GC MGC-803 cells via Human phospho-kinase array. The results showed that RPL31 knockdown inhibited phosphorylation of p70 S6K, PRAS40, RSK1/2, STAT2, STAT5a/b, STAT1 and STAT3, while promoted phosphorylation of Yes (Fig. 5A and B). Moreover, western blotting assay exhibited that in RPL31-harboring MGC-803 cells, Bcl-2, c-Myc and p-Stat3 proteins were considerably downregulated while JAK1 and JAK2 were more expressed than that in shCtrl-harboring cells (Fig. 5C). These findings indicated that JAK-STAT signaling pathway may be involved in the regulation of RPL31 in human GC MGC-803 cells.

3.7. RPL31 knockdown reduces the tumor growth of xenograft in vivo

To further clarify the effect of RPL31 on GC, MGC-803 cells transfected with shRPL31 and shCtrl were injected subcutaneously into nude mice to establish an *in vivo* xenograft tumor model. By monitoring the tumor growth after injection, founding that the tumors in the mice of the shCtrl group grew faster than those in the shRPL31 group (Fig. 6A). Fluorescent imaging was captured and the total fluorescence intensity in controls were significantly higher in the *RPL31*-silencing group ($P < 0.05$; Fig. 6B). Not surprisingly, the solid tumors stripped from shRPL31-harboring mice were much lighter than those from controls ($P < 0.001$; Fig. 6C). Afterward, the tumor tissues of each group were biopsied and subjected to IHC staining to reveal the expression of the proliferation marker KI67. Representative images showed that the intensity of KI67 expression in RPL31 knockout group was weaker than that in control group (Fig. 6D). In short, downregulation of RPL31 evoked nonnegligible inhibition in GC tumorigenesis *in vivo*.

4. Discussion

GC is a kind of gastrointestinal malignancy, which needs more effective new therapy to meet the needs of patients [8]. As a ribosomal protein of the large subunit, RPL31 may not be essential for binding of RAC to the ribosome but connected with functioning of the chaperone complex. Thus, RPL31 is considered to play an essential role in multiple cellular processes [16]. A number of studies have reported that RPL31 is abnormally expressed in a variety of human cancers and has the potential to serve as a molecular target [12]. Since the function and clinical value of RPL31 in GC have not been revealed, this study was conducted. In this study, we identified that RPL31 was overexpressed in GC tissues compared with that in para-carcinoma tissues. In both GC clinical samples and cell lines (AGS and MGC-803), RPL31 was found to be highly expressed, which indicated its involvement of tumor progression. According to speculation from data on RPL31-depletion yeast strain, RPL31 deficiency could seriously impair the assembly of ribosomal large subunits and thus cellular normal physiological processes [10]. In this study, detection in cell cycle of experimental cells indicated that RPL31 deficiency blockaded G1/S transition and further interfered cell growth and proliferation in GC cells. The inhibitory effects of RPL31 depletion on tumor cell migration was verified. Moreover, *in vivo* mice experiments verified these *in vitro* findings and the pro-tumor functions of RPL31. Similarly, a previous study has demonstrated that another ribosomal protein, RPL32, which is also a component of the 60 S subunit, is upregulated in human breast cancer cells. Knocking down RPL32 could result in inhibition of migration and invasion of breast cancer cells both *in vitro* and *in vivo* [18]. Taken together, downregulating of RPL31 could significantly promote cell apoptosis but inhibit cell growth and migration.

In basis of our preliminary exploration of underlying mechanism, we found that RPL31-mediated promotion in tumor development

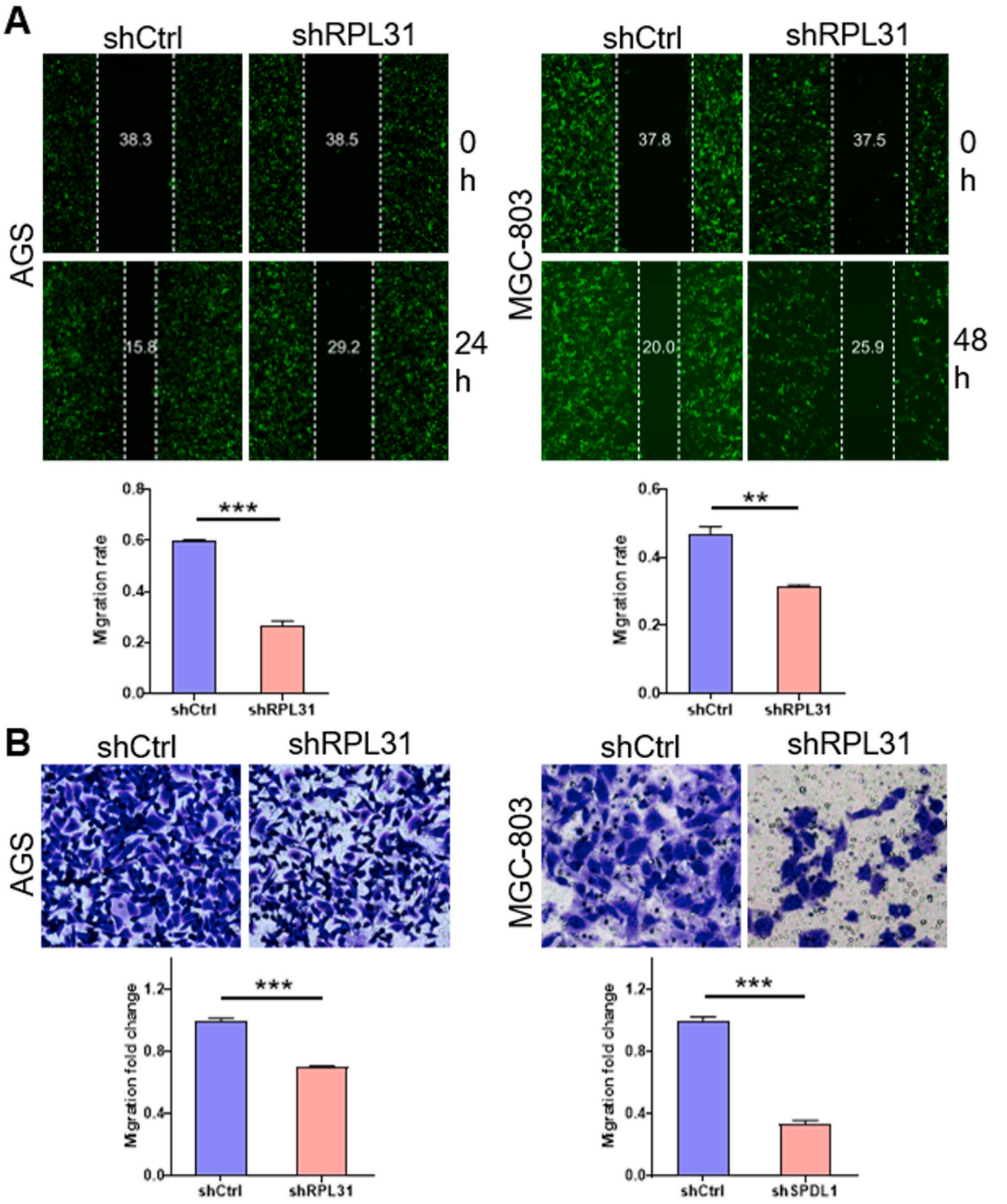

Fig. 4. RPL31 knockdown inhibits migration of GC cells. (A) The migration rates and comparisons between shRPL31-harboring and negative groups in AGS and MGC-803 cell lines from wound-healing assay. **(B)** The representative staining photographs and the migration ability of cells in shRPL31-harboring and negative groups of AGS and MGC-803 cell lines demonstrated by Transwell assay. $^{**}P < 0.01$, $^{***}P < 0.001$.

may involve in the regulation of JAK-STAT signaling pathway. The JAK-STAT pathway is one of the best understood signal transduction cascades which is deeply involved in cellular inflammation-mediated pathological processes through transducing downstream cytokines and further influences the pathogenesis of mammalian immune-mediated disease [19,20]. Growing numbers of publications

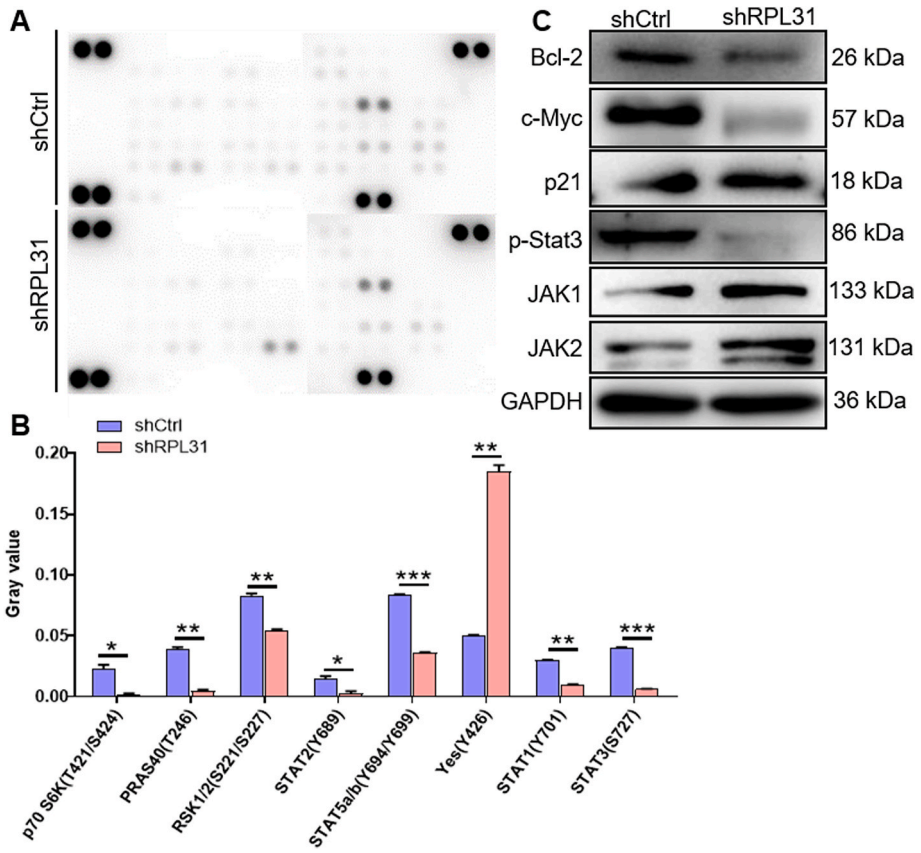

Fig. 5. The underlying regulating mechanism of RPL31 in GC cells. (A–B) The comparison of protein levels in shRPL31 and shCtrl groups of MGC-803 cells resulted from Human phospho-kinase array. **(C)** The changes in expression of Bcl-2, c-Myc, P21, p-Stat3, JAK1 and JAK2 as a result of RPL31 knockdown. Notably, full and non-adjusted images are available in the Supplemental materials folder. $*P < 0.05$, $**P < 0.01$, $***P < 0.001$.

have reported activation of JAK kinases and activators of transcription (STATs) in human oncogene-transformed cells and cancers cells [21,22]. In some human cancers and cancer-derived cell lines, overexpression and activation of STAT3 contributed to high cell proliferation, inhibition of cell differentiation and maturation [23]. Moreover, there is a high incidence of constitutive activation of STAT1, STAT3 and STAT5 in most tumors [24]. In our research, the results of Human phospho-kinase array and western blotting assay revealed suppression of phosphorylation activation of STAT1, STAT2, STAT3 and STAT5 when RPL31 expression was blocked. The elevated JAK1 and JAK2 levels were also indicated in shRPL31-harboring MGC-803 cells compared with shCtrl-harboring cells. We suggested that overexpressed RPL31 mediated GC cell growth and tumor development via regulation of JAK-STAT pathway. Future studies are required to clarify the precise role of RPL31 in JAK-STAT signaling and potential inflammatory response of GC cells.

Of note, there are some limitations to the current study. For instance, the sample size of clinical GC patients is only a small part, and further sample collection should be expanded to verify the results of this study. Secondly, we have only preliminarily revealed that RPL31 knockdown can cause abnormalities in the downstream pathway, but the underlying mechanism of its regulation of GC remains unelucidated, which requires further investigation.

In conclusion, RPL31 was abundantly expressed in GC tissues and cell lines. In addition, RPL31 expression was positively correlated with the extent of tumor infiltrate of GC patients. Functionally, silencing RPL31 in AGS and MGC-803 cells significantly limited the ability of proliferation and migration, promoted cell apoptosis. Consistently, RPL31-knockdown GC cells inhibited the growth of xenografts in mice. Moreover, preliminary analysis on the downstream regulation mechanism revealed that RPL31 functioned as a tumor promoter through targeting JAK-STAT signaling pathway. In conclusion, inhibition of abnormally high expression of RPL31 in GC may be a potential therapeutic strategy for this disease.

Author contribution statement

Fang Wu: Conceived and designed the experiments; Performed the experiments; Wrote the paper.
Yangyang Liu: Performed the experiments.
Shenglin Hu: Analyzed and interpreted the data.
Canrong Lu: Conceived and designed the experiments; Contributed reagents, materials, analysis tools or data.

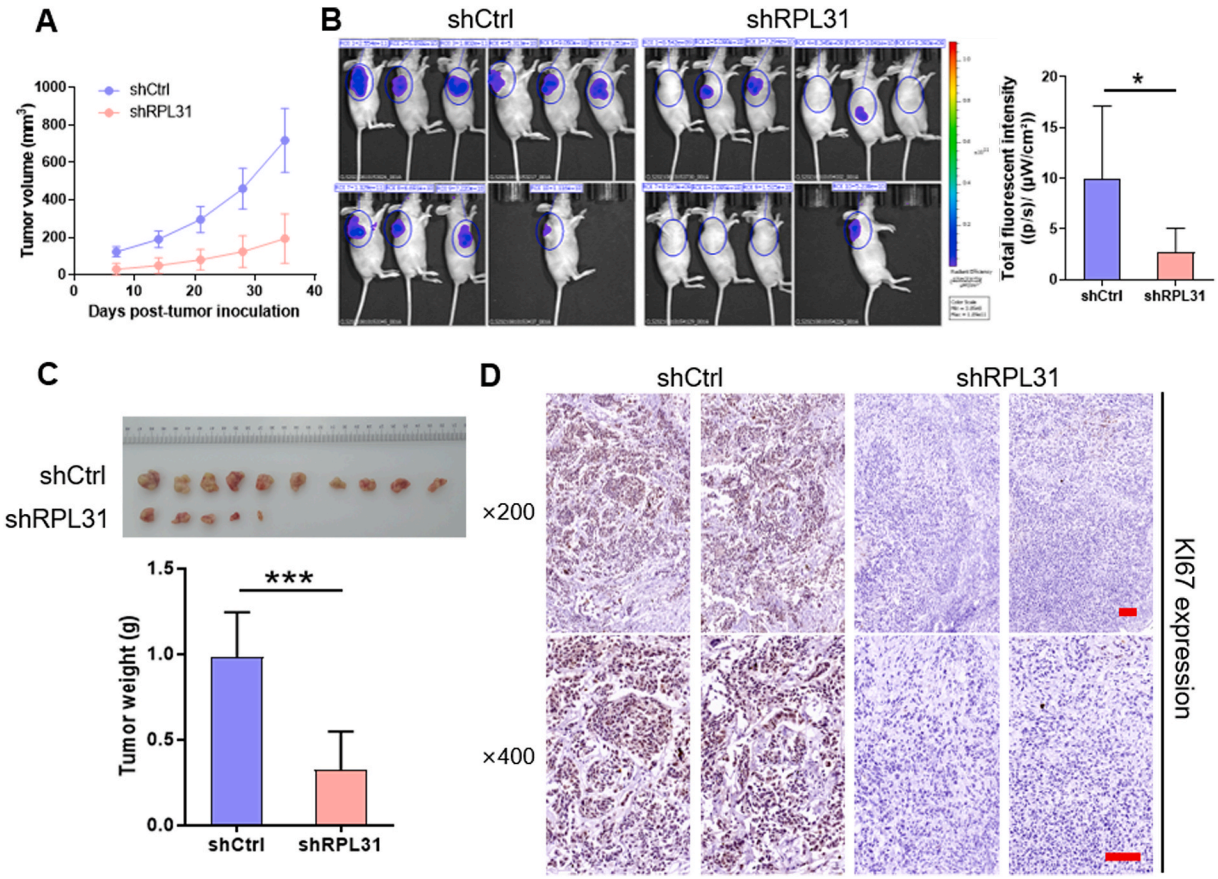

Fig. 6. Depletion of RPL31 imposes restrictions on tumor growth *in vivo*. **(A)** The growing volume of transplanted tumor after injecting shRPL31 and shCtrl groups of MGC-803 cells. **(B)** The fluorescence images and the comparison of total fluorescence intensity of experimental animals between shRPL31 and shCtrl groups. **(C)** The separated xenograft tumors from experimental animals and the comparison in tumor weight between shRPL31 and shCtrl groups. **(D)** The representative images of xenograft tumors after KI67 staining. $^{*}P < 0.05$, $^{***}P < 0.001$.

Funding statement

This research did not receive any specific grant from funding agencies in the public, commercial, or not-for-profit sectors.

Data availability statement

The data set supporting the results of this article are included within the article.

Declaration of interest's statement

The authors declare that they have no known competing financial interests or personal relationships that could have appeared to influence the work reported in this paper.

Appendix A. Supplementary data

Supplementary data related to this article can be found at https://doi.org/10.1016/j.heliyon.2023.e13076.

References

[1] R.L. Siegel, et al., Cancer statistics, 2021, CA A Cancer J. Clin. 71 (1) (2021) 7–33.
[2] N. Rana, et al., Socio-demographic disparities in gastric adenocarcinoma: a population-based study, Cancers 12 (1) (2020).
[3] M. Plummer, et al., Global burden of gastric cancer attributable to Helicobacter pylori, Int. J. Cancer 136 (2) (2015) 487–490.

[4] X. Liang, et al., Treatment strategies for metastatic gastric cancer: chemotherapy, palliative surgery or radiotherapy? Future Oncol. 16 (5) (2020) 91–102.
[5] J. Kozak, et al., Inhibition or reversal of the epithelial-mesenchymal transition in gastric cancer: pharmacological approaches, Int. J. Mol. Sci. 22 (1) (2020).
[6] S.S. Joshi, B.D. Badgwell, Current treatment and recent progress in gastric cancer, CA A Cancer J. Clin. 71 (3) (2021) 264–279.
[7] J.A. Ajani, et al., Gastric cancer, version 2.2022, NCCN clinical practice Guidelines in oncology, J. Natl. Compr. Cancer Netw. 20 (2) (2022) 167–192.
[8] I. Mokadem, et al., Recurrence after preoperative chemotherapy and surgery for gastric adenocarcinoma: a multicenter study, Gastric Cancer 22 (6) (2019) 1263–1273.
[9] D. Ruggero, P.P. Pandolfi, Does the ribosome translate cancer? Nat. Rev. Cancer 3 (3) (2003) 179–192.
[10] K. Peisker, et al., Ribosome-associated complex binds to ribosomes in close proximity of Rpl31 at the exit of the polypeptide tunnel in yeast, Mol. Biol. Cell 19 (12) (2008) 5279–5288.
[11] G. Yusupova, M. Yusupov, High-resolution structure of the eukaryotic 80S ribosome, Annu. Rev. Biochem. 83 (2014) 467–486.
[12] K.A. Chester, et al., Identification of a human ribosomal protein mRNA with increased expression in colorectal tumours, Biochim. Biophys. Acta 1009 (3) (1989) 297–300.
[13] J. Shu, X.J. He, G.C. Li, Construction of cDNA library from NPC tissue and screening of antigenic genes, Cell. Mol. Immunol. 3 (1) (2006) 53–57.
[14] X.L. Su, et al., Expression, purification, and evaluation for anticancer activity of ribosomal protein L31 gene (RPL31) from the giant panda (Ailuropoda melanoleuca), Mol. Biol. Rep. 39 (9) (2012) 8945–8954.
[15] G. Sharen, et al., Silencing eL31 suppresses the progression of colorectal cancer via targeting DEPDC1, J. Transl. Med. 20 (1) (2022) 493.
[16] Y. Maruyama, et al., Short hairpin RNA library-based functional screening identified ribosomal protein L31 that modulates prostate cancer cell growth via p53 pathway, PLoS One 9 (10) (2014) e108743.
[17] H. In, et al., Validation of the 8th edition of the AJCC TNM staging system for gastric cancer using the national cancer database, Ann. Surg Oncol. 24 (12) (2017) 3683–3691.
[18] L. Xu, et al., Biological effect of ribosomal protein L32 on human breast cancer cell behavior, Mol. Med. Rep. 22 (3) (2020) 2478–2486.
[19] T. Iwamoto, et al., The JAK-inhibitor, JAB/SOCS-1 selectively inhibits cytokine-induced, but not v-Src induced JAK-STAT activation, Oncogene 19 (41) (2000) 4795–4801.
[20] A.V. Villarino, Y. Kanno, J.J. O'Shea, Mechanisms and consequences of Jak-STAT signaling in the immune system, Nat. Immunol. 18 (4) (2017) 374–384.
[21] P.J. Murray, The JAK-STAT signaling pathway: input and output integration, J. Immunol. 178 (5) (2007) 2623–2629.
[22] S.Y. Moon, et al., Phytochemicals targeting JAK-STAT pathways in inflammatory bowel disease: insights from animal models, Molecules 26 (9) (2021).
[23] S. Abroun, et al., STATs: an old story, yet mesmerizing, Cell J. 17 (3) (2015) 395–411.
[24] S. Banerjee, et al., JAK-STAT signaling as a target for inflammatory and autoimmune diseases: current and future prospects, Drugs 77 (5) (2017) 521–546.